

GALAXY STELLAR MASS ASSEMBLY: SUPERNOVA FEEDBACK, PHOTO-IONIZATION AND NO-STAR-FORMING GAS RESERVOIR.

M. Cousin¹

Abstract. Semi-analytical models are currently the best way to understand the formation of galaxies within the cosmic dark-matter structures. While they fairly well reproduce the local stellar mass functions, they fail to match observations at high redshift. The inconsistency indicates that the gas accretion in galaxies and the transformation of gas into stars, are not well followed. With a new SAM: eGalICS, we explore the impacts of classical mechanisms (supernova feedback, photo-ionization) onto the stellar mass assembly. Even with a strong efficiency, these two processes cannot explain the observed stellar mass function and star formation rate distribution. We introduce an ad-hoc modification of the standard paradigm, based on the presence of a no-star-forming gas component in galaxy discs. We introduce this reservoir to generate a delay between the accretion of the gas and the star formation process. The new stellar mass function and SFR distributions are in good agreement with observations.

Keywords: Galaxies: formation - Galaxies: evolution - Cosmology: dark-matter haloes

1 Introduction

Cosmological models based on the Λ -CDM paradigm have proved remarkably successful at explaining the origin and evolution of structures in the Universe. The description of smaller scales (galaxies) is more problematic. Twenty years ago, Kauffmann et al. (1993) pointed out the so-called substructure problem. Indeed the large amount of power on small scales in the $\Lambda - CDM$ paradigm generates an over-estimate of the number of small objects (with properties close to dwarf galaxies). The over-density of substructures is clearly seen in N-body simulations at low redshift ($z \simeq 0$). Dark matter haloes with mass comparable to that of our Galaxy ($M_h \simeq 10^{12} M_\odot$) contain more than one hundred substructures. On the contrary, the observations of the Local Group count at most fifty satellite galaxies. This effect is even more problematic at high redshift ($z > 1$). Indeed, coupled with the poor understanding of the star formation process in these small haloes, the standard scenario produces a large excess of stellar mass in low-mass structures (Guo et al. 2011).

To limit the number of dwarf galaxies, galaxy formation models such as semi-analytical model (SAM) or cosmological hydrodynamic simulations, invoke gas photoionization and strong supernova feedback (Efstathiou 1992; Shapiro et al. 1994; Babul & Rees 1992; Quinn et al. 1996; Thoul & Weinberg 1996; Bullock et al. 2000; Gnedin 2000; Benson et al. 2002; Somerville 2002; Croton et al. 2006; Hoefl et al. 2006; Okamoto et al. 2008; Somerville et al. 2008, 2012).

We use a revised version of the GalICS semi-analytical model (SAM) (Cousin et al 2014-b). This new version include a description of the baryonic physic based on the most recent prescriptions extracted from analytical works and/or hydrodynamic simulations. With this SAM we explore the impacts of classical photoionization and supernova (SN)-feedback recipes on fundamental the stellar mass function (SMF).

We show that the basic models fail to reproduce these kinds of measurements, and propose the existence of a *no-star-forming* gas reservoir in galaxy discs to reconcile the models with the observations.

This conclusion is based on the analysis of a set of four different prescriptions of star-formation regulation processes. These four different models are listed in the table 1. In the first model, m_0 , the star formation

¹ Institut d'Astrophysique Spatiale, Universit  Paris-Sud 11, bat 121, 91405 ORSAY

Model	Definitions / Comments	Colour plots
m_0	Okamoto et al. (2008), without (sn/agn)-feedback	red
m_1	Okamoto et al. (2008) photoionization and our sn-feedback processes (<i>reference</i>)	orange
m_2	Gnedin (2000) photoionization and our sn-feedback processes	green
m_3	<i>reference</i> + <i>no-star-forming</i> gas disc component	purple

Table 1. List of SAMs compared

activity is not regulated. Indeed this first model does not use any feedback or photo-ionization prescription. The model m_1 uses a SN feedback recipe and a photo-ionization model based on the Okamoto et al. (2008) prescription. The model m_2 is based on the same SN model, than model m_1 , but it uses the Gnedin (2000) photoionization prescription. Finally, the last model, m_3 , applies a new model of gas cycle. It assumes the existence of a *no-star-forming* gas reservoir in galaxy discs.

2 Supernovae feedback

In a given stellar population, massive stars evolve quickly and end their life as supernovae. This violent death injects gas and energy in the interstellar medium. The gas is heated and a fraction can be ejected from the galaxy plane and feed the surrounding host-halo phase.

Supernova feedback is therefore a crucial ingredient. In the majority of SAM (e.g. Kauffmann et al. 1993; Cole et al. 1994, 2000; Silk 2003; Hatton et al. 2003; Somerville et al. 2008), and according to some observational studies (e.g. Martin 1999; Heckman et al. 2000; Veilleux et al. 2005), the *SN-reheating* or *SN-ejecta* rate is linked to the star formation rate. As proposed by Dekel & Silk (1986), we computed the ejected mass rate due to supernovae by using kinetic energy conservation. The ejected mass rate $\dot{M}_{ej,SN}$ due to SN is linked to the star formation rate \dot{M}_\star by using the individual supernova kinetic energy $E_{sn,k}$ as follows:

$$\dot{M}_{ej,SN} V_{wind}^2 = 2\varepsilon_{ej}\eta_{sn} E_{sn,k} \dot{M}_\star \quad (2.1)$$

To break the degeneracy between the ejected mass and the velocity of the wind, we must add a constraint on the wind velocity. We rely on Bertone et al. (2005) in which the wind velocity is linked to the star formation rate (Martin 1999). It seems to be independent of the galaxy morphology (Heckman et al. 2000; Frye et al. 2002). We therefore use Eq. 9 in Bertone et al. (2005) to model the wind velocity.

On average, wind velocities obtained with this prescription are larger than in other studies (e.g. Somerville et al. 2008; Dutton & van den Bosch 2009). Indeed it is common to use galaxy escape velocity to describe the wind, which is, for the ejection process, the minimal required value. Therefore, the ejected mass is maximal (see Dutton & van den Bosch (2009), their discussion in Sect.7.3). Consequently, our loading factor ($\dot{M}_{ej,SN}/\dot{M}_\star$) is smaller than in other models and therefore our mean ejected mass is also lower.

The influence of the efficiency value has been tested in the range $\varepsilon_{ej} \in [0.05, 10]$. Obviously a strong increase of the SN-efficiency increases the amount of ejected gas. The star formation activity is therefore reduced but this effect affects only the amplitude and not the shape of the stellar mass function. Moreover, looking at the amplitude, its decrease is not enough to be in agreement with the observations.

Despite the different parameterizations and energy injection scales for supernovae, currently the classical semi-analytical models do not seem to be able to explain the high redshift behaviour of the mass function in the low-mass range (see also Fig. 23 in Guo et al. (2011), and Fig. 11 in Ilbert et al. (2013)). Even if some SAMs, as Somerville et al. (2008), Guo et al. (2011) or Henriques et al. (2013), use a dedicated parametrization, to reproduce the galaxy properties at $z = 0$, it seems that, at high redshift, the low-mass range problem of the stellar-mass function is not only linked to a SN-feedback efficiency calibration. Indeed, Guo et al. (2011) (their Figs. 8 and 23) show that the number of low-mass star-forming galaxies are still larger than that observed.

Note also that a strong increase of the SN-wind efficiency, in low-mass structures, leads to very high mass-loading factors ($\dot{M}_{ej}/\dot{M}_\star > 10$, Henriques et al. (2013) their Fig. 3). Such factors are much larger than those derived from spectroscopic observations (e.g. Sturm et al. 2011; Rubin et al. 2011; Bouché et al. 2012) even if the measurement of this parameter is difficult and is currently performed on massive systems.

3 Photoionization

Originally proposed by Doroshkevich et al. (1967), photoionization has been developed in the *CDM* paradigm by Couchman & Rees (1986), Ikeuchi (1986), and Rees (1986). The idea is quite simple: the ultraviolet (UV) background generated by the quasars and first generations of stars heats the gas. In the small structures, the temperature reached by the gas is then too high, preventing it to collapse into dark matter haloes. The accretion of the gas on the galaxies, and thus the star formation, is thus reduced.

In our hybrid SAMs, the baryonic mass is added progressively following the dark-matter smooth accretion:

$$\dot{M}_b = f_b^{ph-ion}(M_h, z) \dot{M}_{dm} \quad (3.1)$$

where

$$f_b^{ph-ion}(M_h, z) = \langle f_b \rangle \left[1 + (2^{\alpha/3} - 1) \left(\frac{M_h}{M_c(z)} \right)^{-\alpha} \right]^{-3/\alpha} \quad (3.2)$$

In this definition, $\langle f_b \rangle = 0.18$ is the universal baryonic fraction, M_h the dark matter halo mass, and $M_c(z)$ the filtering mass corresponding to the mass where the halo lost half of its baryons. Finally, α is a free parameter that mainly controls the slope of the transition. In our case, we use the Okamoto et al. (2008) prescription ($\alpha = 2$ and $M_c(z) = 8.22 \times 10^9 \exp(-0.7z) [M_\odot]$).

We consider that the photoionization effect is important when $f_b^{ph-ion} < 0.5 \langle f_b \rangle$. In this context, the significant decrease of $f_b^{ph-ion} / \langle f_b \rangle$ appears for the mass resolution ($M_h^{min} = 1.707 \times 10^9 M_\odot$) only for redshift $z < 1$. In this case, the gas heating due to the UV background cannot affect, at high redshift, the baryonic assembly of small structures. Some other SAM (e.g. , (e.g. Benson et al. 2002; Somerville 2002; Croton et al. 2006; Hoesft et al. 2006; Okamoto et al. 2008; Somerville et al. 2008, 2012) use a different parametrization based on Gnedin (2000) ($\alpha = 1$ and with a different filtering mass). This other he Gnedin (2000) prescription reduces more the stellar mass formed in the small dark matter mass regime than the Okamoto et al. (2008) prescription. Indeed, with this model, photoionization starts to play a role at $z \simeq 8$.

4 An ad-hoc recipe to reconcile models and observations

At high redshift ($z > 1$), as shown in Fig. 1, the amplitude of the faint-end of the stellar mass function is dramatically overestimated by the models (m_0 , m_1 and m_2). This result is consistent with the overestimate of stellar mass in low-mass dark matter haloes: small structures form too many stars. In general, this problem is addressed by a strong SN-feedback and/or photoionization. As shown previously, photoionization and SN-feedback cannot be sufficient to reduce significantly the star formation in low-mass objects. Strong feedback models give some good integrated (at $z \simeq 0$) results (Guo et al. 2011; De Lucia & Blaizot 2007) but fail at higher redshift (see Ilbert et al. 2013, their Fig. 11).

We propose in this section a strong modification of the implementation of the star-formation mechanism in our semi-analytical model to try to reconcile models and observations.

When accreted on the galaxy disc, the surface density of fresh gas (considered as homogeneously distributed) is low. Progressively the gas, controlled by the turbulence and gravity energy balance, is more and more structured (Kritsuk & Norman 2011). The energy injected by the accretion process must be dissipated before star-formation process can start. As the dissipation scale is much smaller than the energy injection scale, we assume that the energy cascade introduces a delay between the accretion time and the star formation time.

To model this process, we introduce in our model m_3 a new gas component in galaxy discs: the *no-star-forming* gas. The delay between the accretion time of fresh gas and the time when this gas is converted into stars is modelled by a transfer rate between the *no-star-forming* gas and the *star-forming* gas reservoir (g^*) that follows:

$$\dot{M}_{g^*,in} = \dot{M}_{g,out} = \varepsilon_\star \min \left[1, \left(\frac{M_h}{10^{12} M_\odot} \right)^3 \right] \frac{M_g}{t_{dyn}} \quad (4.1)$$

where M_g is the mass of *no-star-forming* gas, t_{dyn} is the disc dynamical time and $\varepsilon_\star = 0.02$ an efficiency parameter, identical to the star formation efficiency used in standard SAM. This conversion rate has not been defined to follow explicitly ISM physic but is calibrated to reproduce the stellar-to-halo mass-relation (SHMR) (e.g. Leauthaud et al. 2012; Moster et al. 2010; Behroozi et al. 2010; Béthermin et al. 2012). This formulation has no other purpose than to highlight the order of magnitude of the regulation process that has to be introduced.

5 The stellar/gas-mass function

5.1 The stellar-mass function

We show in Figs 1 and 2 the stellar-mass functions predicted by our models. In Fig 1 are shown *standard* models, m_0 (red), without regulation process, m_1 (orange) with a SN feedback model and the Okamoto et al. (2008) photo-ionization prescription and m_2 (green) with the same SN feedback model but with the Gnedin (2000) photo-ionization prescription. Model outputs are compared with observational data from Ilbert et al. (2010), Ilbert et al. (2013), Yang et al. (2009) and Caputi et al. (2011).

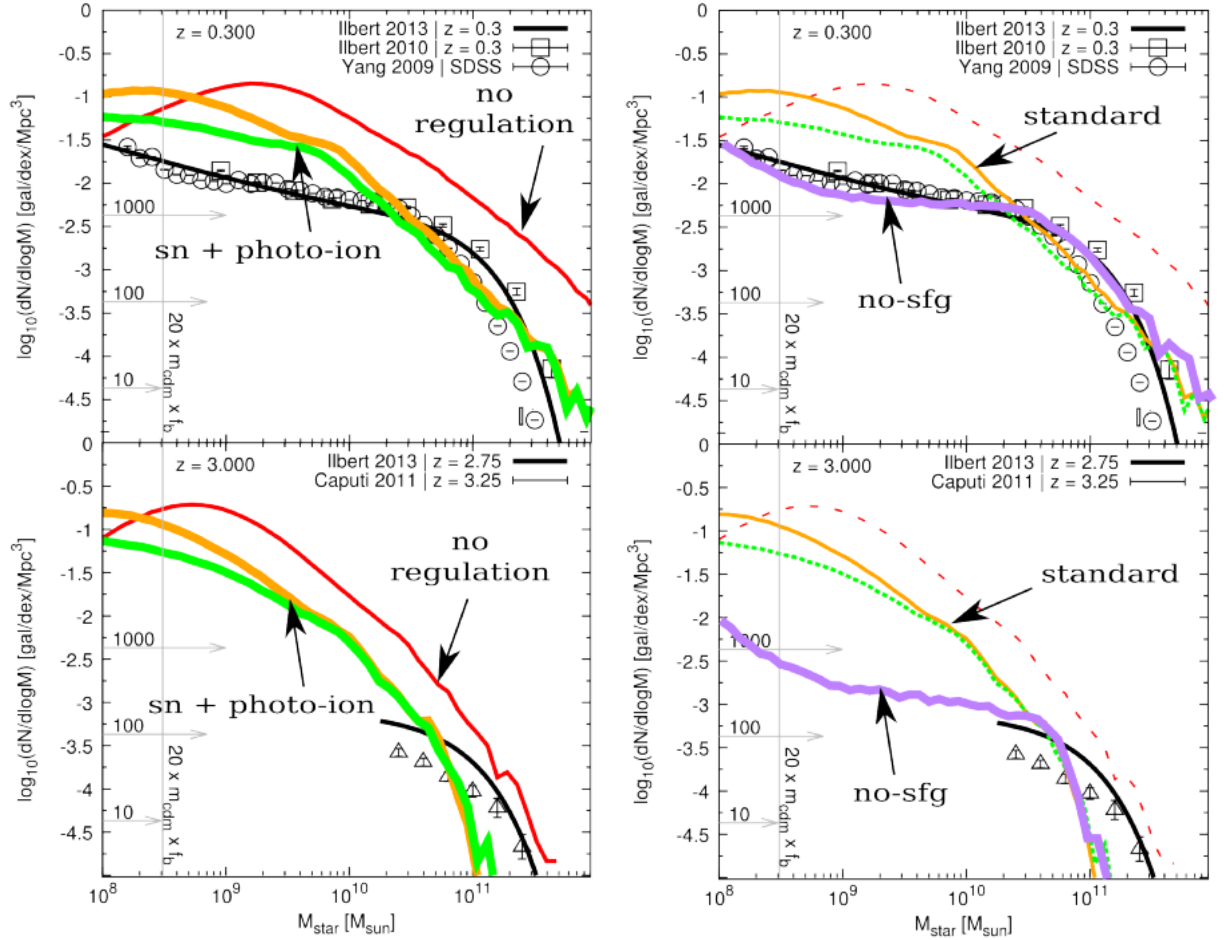


Fig. 1. Left: Stellar mass functions for two different redshift bins, $z = 0.3$ (top panel) and $z = 3.0$ (bottom panel) and for our standard models, m_0 (red), m_1 (orange) and m_2 (green). **Right:** Stellar mass functions extracted from our *ad-hoc* model (purple) for two different redshift bins, $z = 0.3$ (top panel) and $z = 3.0$ (bottom panel). Other model m_0 (red), m_1 (orange) and m_2 (green) are recalled. **Both:** We compare our results with Ilbert et al. (2010, 2013) (squares), Yang et al. (2009) (circles) and Caputi et al. (2011) (triangles) observations. The horizontal arrows show the link between the density and the number of haloes in our simulation volume.

It is clear that models m_0 , m_1 and m_2 fail to reproduce the low-mass end of the stellar mass function. The disagreement is both on the amplitude (one order of magnitude higher at low mass) and on the shape of the mass function. Note that the discrepancy increase with the redshift.

With the *ad-hoc* model (purple), in the low mass range, the levels of the stellar mass functions are in good agreement with observations for a wide range of stellar masses. This indicates that only a strong modification (a decrease in our case) of the mass of gas instantaneously available to form stars, allows to modulate the star formation activity in low mass structures and to reconcile SAM with the observations.

Concerning the high-mass end of the stellar-mass function, all models under-predict the number of massive galaxies. For $z = 4$ and $z = 3$ the comparison with Ilbert et al. (2010) and Ilbert et al. (2013) observational mass functions indicate that the massive galaxies in our models are two time less massive than the observed distribution. This is also observed in other recent SAMs (see e.g., Henriques et al. 2013, their Figs. 4-5-6, and Guo et al. 2011, their Fig. 23). The only way to reconcile models and observation in this high-mass regime is to consider a model without any regulation mechanism (model m_0).

5.2 The gas-mass function

In our *ad-hoc* model, we have chosen to modify the standard star formation paradigm, through the introduction of a delay between gas accretion and star formation. The step during which the *no-star-forming* gas is converted into *star-forming* gas strongly reduces the star formation activity, and therefore the stellar mass building-up.

In Fig. 2, we show the predicted gas-mass functions, together with the local HI mass function computed by Zwaan et al. (2005), and the molecular gas mass function coming from Berta et al. (2013). The gas-mass functions extracted from our models are computed using all galaxies contained in our simulated volume, and taking into account the total gas mass in galaxy discs.

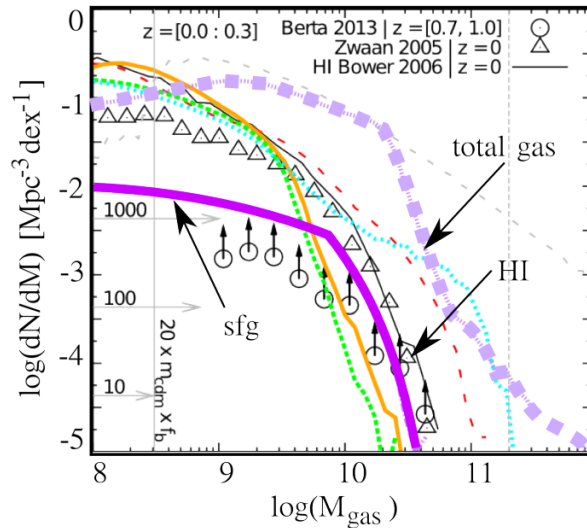


Fig. 2. Gas mass functions predicted by our SAMs. The colour code is detailed in Table 1. In the case of m_4 , we plot the total (*star-forming* + *no-star-forming*) and the *star-forming* gas mass function. We compare our results with the molecular gas mass function computed by Berta et al. (2013) (lower limits, circles) and with the local HI mass function computed by Zwaan et al. (2005) (triangles). The black solid line shows the HI mass function predicted by Lagos et al. (2011), using Bower et al. (2006) SAM. The horizontal arrows show the link between the density and the number of haloes in our simulation volume.

The gas-mass functions predicted by our reference model m_1 and its variation (m_2) are very close. Indeed, the two models use the same prescription for gas ejection. In the case of the new model m_3 , we plot together in Fig. 2 the total and the *star-forming* gas-mass function. As expected, the amount of total gas in m_4 is larger than in the reference model m_1 or its variations (m_2).

We also show in Fig. 2 the HI-mass function derived by Lagos et al. (2011) using the SAM of Bower et al. (2006). At first order, it is comparable to the mass-function evolution from our reference model m_1 , which is reassuring and expected.

At $z \simeq 0$, the amount of total gas predicted by m_4 is larger than the measurement of the HI gas and the lower values of the molecular gas. Independently of each other, the HI and the molecular gas represent only a fraction of the total gas mass contained in a galaxy. However, we can note that for the high-mass range, the *star-forming* gas mass function predicted by m_3 is in good agreement with the HI mass function measured by Zwaan et al. (2005). Even if the total gas mass predicted by m_3 seems large, without any measurement of this total mass, it is difficult to conclude. The total gas mass function appears today as one of the key observables which will allow us to determine the optimal efficiency of gas ejection process and star formation.

6 Discussion, conclusion

We have presented different processes which act on galaxy formation, and more precisely on the star formation activity. We have tested two photoionization models and we have applied a supernovae feedback models. We showed that classical models fail to reproduce the faint-end of the stellar-mass function. They over-predict the stellar mass in the low mass dark matter haloes ($M_h < 10^{10} M_\odot$). Even when a strong photoionization and SN-feedback are used, the models form too many stars in the low-mass range. Moreover, recent observations indicate that the loading factors (\dot{M}_{ej}/\dot{M}_*) are much smaller than those predicted by such models. A strong SN-feedback generates a strong decrease of the amount of gas, that has to be compensated at low z , for example by some gas reincorporation (Henriques et al. (2013)). Such a problem in the low-mass structures is invariably present, even in the most recent SAMs (Guo et al. 2011; Bower et al. 2012; Weinmann et al. 2012), and as explained by Henriques et al. (2013) can thus be viewed as a generic problem.

In addition to these standard models, we have proposed an other model in which we have strongly limited the star formation efficiency in low-mass haloes. This model is based on a 2-phase gaseous disc with, on the one hand the *star-forming* gas, and on the other hand, the *no-star-forming* gas. This *ad-hoc* modification leads to very good results mainly for the stellar-mass functions. The gas-mass function predicted by the *ad-hoc* model may indicate that galaxies have a gas content that is too large, even if the comparison with observations is difficult as the total gas mass function is not known. In the future, the measurement of the gas mass function will be a key observable that will constrain the balance between the ejection process and gas regulation in galaxies.

We acknowledge financial support from "Programme National de Cosmologie and Galaxies" (PNCG) of CNRS/INSU, France.

References

- Babul, A. & Rees, M. J. 1992, MNRAS, 255, 346
 Behroozi, P. S., Conroy, C., & Wechsler, R. H. 2010, ApJ, 717, 379
 Benson, A. J., Lacey, C. G., Baugh, C. M., Cole, S., & Frenk, C. S. 2002, MNRAS, 333, 156
 Berta, S., Lutz, D., Nordon, R., et al. 2013, A&A, 555, L8
 Bertone, S., Stoehr, F., & White, S. D. M. 2005, MNRAS, 359, 1201
 Béthermin, M., Doré, O., & Lagache, G. 2012, A&A, 537, L5
 Bouché, N., Hohensee, W., Vargas, R., et al. 2012, MNRAS, 426, 801
 Bower, R. G., Benson, A. J., & Crain, R. A. 2012, MNRAS, 422, 2816
 Bower, R. G., Benson, A. J., Malbon, R., et al. 2006, MNRAS, 370, 645
 Bullock, J. S., Kravtsov, A. V., & Weinberg, D. H. 2000, ApJ, 539, 517
 Caputi, K. I., Cirasuolo, M., Dunlop, J. S., et al. 2011, MNRAS, 413, 162
 Cole, S., Aragon-Salamanca, A., Frenk, C. S., Navarro, J. F., & Zepf, S. E. 1994, MNRAS, 271, 781
 Cole, S., Lacey, C. G., Baugh, C. M., & Frenk, C. S. 2000, MNRAS, 319, 168
 Couchman, H. M. P. & Rees, M. J. 1986, MNRAS, 221, 53
 Croton, D. J., Springel, V., White, S. D. M., et al. 2006, MNRAS, 365, 11
 De Lucia, G. & Blaizot, J. 2007, MNRAS, 375, 2
 Dekel, A. & Silk, J. 1986, ApJ, 303, 39
 Doroshkevich, A. G., Zel'dovich, Y. B., & Novikov, I. D. 1967, Soviet Ast., 11, 233
 Dutton, A. A. & van den Bosch, F. C. 2009, MNRAS, 396, 141
 Efstathiou, G. 1992, MNRAS, 256, 43P
 Frye, B., Broadhurst, T., & Benítez, N. 2002, ApJ, 568, 558
 Gnedin, N. Y. 2000, ApJ, 542, 535
 Guo, Q., White, S., Boylan-Kolchin, M., et al. 2011, MNRAS, 413, 101
 Hatton, S., Devriendt, J. E. G., Ninin, S., et al. 2003, MNRAS, 343, 75
 Heckman, T. M., Lehnert, M. D., Strickland, D. K., & Armus, L. 2000, ApJS, 129, 493
 Henriques, B. M. B., White, S. D. M., Thomas, P. A., et al. 2013, MNRAS, 431, 3373
 Hoft, M., Yepes, G., Gottlöber, S., & Springel, V. 2006, MNRAS, 371, 401
 Ikeuchi, S. 1986, Ap&SS, 118, 509

- Ilbert, O., McCracken, H. J., Le Fevre, O., et al. 2013, ArXiv e-prints
- Ilbert, O., Salvato, M., Le Floch, E., et al. 2010, ApJ, 709, 644
- Kauffmann, G., White, S. D. M., & Guiderdoni, B. 1993, MNRAS, 264, 201
- Kritsuk, A. G. & Norman, M. L. 2011, ArXiv e-prints
- Lagos, C. D. P., Baugh, C. M., Lacey, C. G., et al. 2011, MNRAS, 418, 1649
- Leauthaud, A., Tinker, J., Bundy, K., et al. 2012, ApJ, 744, 159
- Martin, C. L. 1999, ApJ, 513, 156
- Moster, B. P., Somerville, R. S., Maulbetsch, C., et al. 2010, ApJ, 710, 903
- Okamoto, T., Gao, L., & Theuns, T. 2008, MNRAS, 390, 920
- Quinn, T., Katz, N., & Efstathiou, G. 1996, MNRAS, 278, L49
- Rees, M. J. 1986, MNRAS, 218, 25P
- Rubin, K. H. R., Prochaska, J. X., Ménard, B., et al. 2011, ApJ, 728, 55
- Shapiro, P. R., Giroux, M. L., & Babul, A. 1994, ApJ, 427, 25
- Silk, J. 2003, MNRAS, 343, 249
- Somerville, R. S. 2002, ApJ, 572, L23
- Somerville, R. S., Gilmore, R. C., Primack, J. R., & Domínguez, A. 2012, MNRAS, 423, 1992
- Somerville, R. S., Hopkins, P. F., Cox, T. J., Robertson, B. E., & Hernquist, L. 2008, MNRAS, 391, 481
- Sturm, E., González-Alfonso, E., Veilleux, S., et al. 2011, ApJ, 733, L16
- Thoul, A. A. & Weinberg, D. H. 1996, ApJ, 465, 608
- Veilleux, S., Cecil, G., & Bland-Hawthorn, J. 2005, ARA&A, 43, 769
- Weinmann, S. M., Pasquali, A., Oppenheimer, B. D., et al. 2012, MNRAS, 426, 2797
- Yang, X., Mo, H. J., & van den Bosch, F. C. 2009, ApJ, 695, 900
- Zwaan, M. A., Meyer, M. J., Staveley-Smith, L., & Webster, R. L. 2005, MNRAS, 359, L30